International Journal of Engineering & Technology, 8 (1.2) (2019) 206-213

International Journal of Engineering & Technology

Website: www.sciencepubco.com/index.php/IJET

Research paper

Prostate Cancer Classification Technique on Pelvis CT Images

Uzair Sahrin[1]*, Siti Norul Huda Sheikh Abdullah[2], Khairuddin Omar[3], Afzan Adam[4], Syazarina Sharis[5]

[1,3,4]Center for Artificial Intelligence Technology, Faculty of Information Science & Technology,
The National University of Malaysia, Selangor, Malaysia
[2]Center for Cyber Security, Faculty of Information Science & Technology,
The National University of Malaysia, Selangor, Malaysia
[5]UKM Medical Centre, Jalan Yaacob Latif, Bandar Tun Razak
Cheras, Kuala Lumpur Malaysia.
**Corresponding author E-mail: uzairadif@yahoo.com*

Abstract

Prostate cancer is one of the commonest cancer found: the forth in Malaysia and sixth in the planet with 307 000 mortalities in 2012. Early detection is important to reduce the death rate; thus this research is carried out to develop an automated prostate cancer classification from the bone scan of pelvis CT images. Preliminary experiment has been carried out using real images from Hospital Chancellor Tuanku Muhriz (formerly known as UKM Medical Center) database. The detection algorithm was developed and compared between Random Forest and Logistic Regression classification of normal and abnormal cancerous prostate image. Furthermore, random tree was selected as the mining technique to model the knowledge in radiology department in predicting the level of prostate cancer severity. A total of 51 cases of prostate cancer patients with 2 urologists, a radiologist and an expert on pathology of PPUKM actively involved in the development of the expert system. The classification has achieved 90% accuracy percentage with 10-fold cross validation technique with Logistic Regression. In addition, the expert system grading on test set has achieved 96% accuracy with the same learning technique.

Keywords: *bone scan classification , cancer detection, cancer expert system,.*

1. Introduction

The American Cancer Society has expected 180 890 new cases with 26 120 deaths from prostate cancer alone for 2016. The number shows that prostate cancer is one of the commonest cancer found, and placed sixth in the world (number of new cases). In Malaysia, it is the 4th most detected cancer for men's [1] where 15.8 percent are Chinese, 14.8 percent are Indian and 7.7 percent are Malays [2].
Figure 1(a) shows reported cancer cases in Malaysia for the year 2014, where 1186 cases are prostate cancer. This is 3 times higher than 2007 where only 502 cases were reported in National Cancer Registry. Figure 1(b) on the other hand, shows the comparison of death rate caused by cancer and the newly diagnosed cancer cases in United States (34.5%), United Kingdom (48.2%) and Malaysia (57.9%).
Similar with other cancer, early detection means the treatment has higher chance of healing and may saves lives [3]. However, detected prostate cancer cases in Malaysia usually has already reached a severe stage where it has spread, and treatment options are limited [4]. Therefore, there is a pressure need to increase the public awareness as well as automated early cancer detection. A few researches have been carried out for this purpose with embedded approach of artificial intelligence and machine learning [5,6]. On top of that, image processing techniques has been implemented to accurately help diagnose and monitor the cancer progression [7]. The latest trends are computerized pre-cancerous tissue condition known as dysplasia, from the esophagus histopathology images [8,9]. Other research using histopathology images are in brain and blood cancer, as well as measuring the estimation of aggressive cancer cell spreading [10] and prostate cancer grading with Gleason Score [11]. Apart from these, radiology images were still used for diagnosing and detecting area of cancer in brain [12,13], breast [14] and cancer classification [15].
The process of diagnosing prostate cancer is tricky because it involves an unknown tumor [6]. Thus, diagnosing a prostate cancer is carried out based on symptoms, physical rectum examination and the readings of certain prostatic antigen (PSA) in blood sample. On top of these, Partin Table has been widely used in Europe and North America as a guide to choose a treatment [5]. This table which was last updated in 2007, combines the probability of pre-PSA operation with TN Mand Gleason score to produce the final pathology outcome.
Apart from these, diagnosing based on individual factor using various logistic regression (LR) and recurrent neural network (RNN) has been developed since 1994 [6]. [5] reported that many researchers use the complementary of RNN, LR and Genetic Algorithm to increase the system performance. One of the example is the implementation of Neuro-Fuzzy and Genetic-Fuzzy system to grade prostate cancer and diagnosing breast cancer. The Genetic-Fuzzy approach has achieved a high-performance rate [5].
Meanwhile, computerized imaging and image processing systems has also been explored to help medical practitioners in making structure, semi-structured or unstructured decision. The interest in this problem and all these ongoing research has proven prediction modeling to suppress the death toll statistics caused by prostate cancer in Malaysia, as well as the world. that prostate cancer recognition is still relevant for further investigations and development. There are rooms for improved detection, classification as well as

(a)

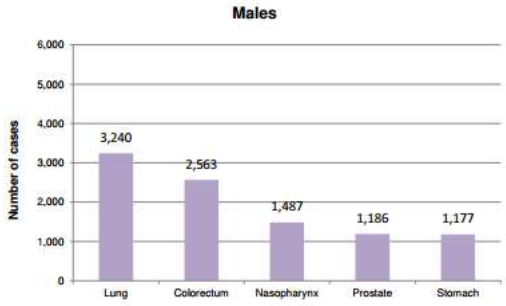

(b)

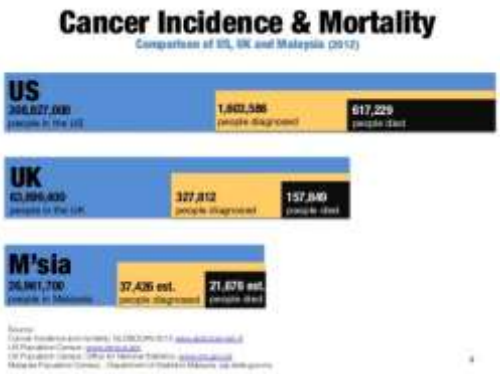

Fig. 1: (a & b) Death rate and number of new cases (Source: World Health Organization Report, 2014 and 2012)

2. Proposed Methodology

This section discusses on data preparation and proposed framework of pelvis bone scan classification system. Usually, patients who are diagnosed with malignant prostate are requested to do follow up checks with bone scanning. The radiologist will observe if any new metastasis existence on bone due to cancer cell proliferation. Localization, symmetry, shape and intensity of each image is important to differentiate abnormal changes due to metastatic or degenerative changes in bone. The pelvis bone scan images were recorded using CT scan machine (Figure 2). It captures sagittal and coronal projections view, and its sequence axes.

Fig. 2: Example of CT Scan machine from HCTM that able to capture the whole projection of human body and tomography images.

This study classifies pelvis bone scan images either normal or abnormal class using two popular classification methods namely Random Forest and Logistic Regression. The framework for pelvis bone scan classification system includes image acquisition, pre-processing, image classification and result projection, as shown in Figure 3.

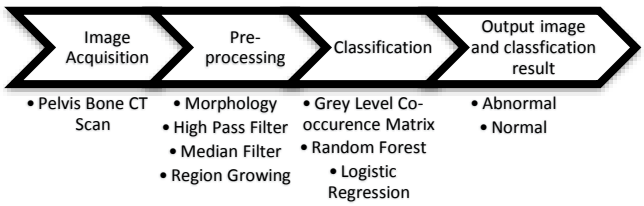

Fig. 3: The framework for pelvis bone scan classification.

2.1 Image acquisition

A collection of 182 bone scan images from 17 patients were obtained after ethical approval dated 22 August 2016 from Hospital Chancellor Tuanku Muhriz (HCTM). This dataset consists of 78 normal images and 104 abnormal images that had been diagnosed as malignant

prostate cancer images. Furthermore, about 7 to 8 images were randomly chosen per patient. Apart from prostate cancer bone scan images, anonymous patient information from Medweb / HCTM PACS server.

2.2 Image pre-processing

Image pre-processing is a very important step in segmentation and classification of images because its affecting the accuracy of extracted image features and eventually, the performance of the classifier. Processes involved in the pre-processing stage includes filtering and region growing. In this study, three image filtering was used for image enhancement; a morphological filter to obtain strong structure, a high pass filter as a frequency domain filter and a median filter as a space domain filter.

2.2.1 Morphological filter

Erosion and dilation are most popular morphological operations. Erosion, also known as 'opening' erodes pixels to moves apart the objects that are too close together, while dilation (or also known as closing) will dilates pixels so that isolated objects that are very near to each other, touches and combined. These filters out small islands and thin filaments of object pixels [16].
The output of the opening operation is combined with original image to perform image subtraction. Image subtraction is a common tool for the analysis of change in pairs of images, used in a wide range of circumstances [17]. The subtraction formula is:

$$Q(i,j) = P2\,(I,j) - P1\,(I,j)\,, \tag{1}$$

where *j* as pixel coordinates, *P1* and *P2* are the pixels of the original image and the opened image, and *Q(i,j)* is the resulted subtracted image.

2.2.2 High pass filter

The foundations of the image enhancement using the high pass filter is the conversion of image in grey color that has been combined with the Fourier transform, frequency components higher. This can be represented as formula as below. Give $\hat{a}$ to show the Fourier transform of the source image, *a*. If *a* shows the result of the Fourier transform function which is low frequency and high for pass, $\hat{\mathrm{h}}$, then the enhanced image of a filter has been filtered through a Fourier transform inversion of $\hat{a}$ and raises the image *g* according to the equation shown:

$$g(x,y) = J^{-1}\{\hat{\mathrm{a}}(u,v).\hat{\mathrm{h}}(u,v)\}\,, \tag{2}$$

where J^{-1} indicates the inverse Fourier transform. High pass transfer function formula originally complete from low pass transfer function. The transition function (transfer function) is based on the following:

$$\hat{\mathrm{h}}(u,v) = \begin{cases} 0 & if\ d\hat{}(u,v) \le d\,, \\ 1 & if\ d\hat{}(u,v) > d\,, \end{cases} \tag{3}$$

where *d* is the nonnegative defined cut off frequency and $d\hat{}(u,v) = (u^2 + v^2)^{1/2}$. Transfer function for Butterworth high pass filter sequentially based on *k* given by:

$$\hat{\mathrm{h}}(u,v) = \begin{cases} \frac{1}{1+c[d/\,d\hat{}\,(u,v)]^{2k}} & if\ (u,v) \neq (0,0)\ , \\ 0 & if\ (u,v) = (0,0)\ , \end{cases} \tag{4}$$

where *c* is a fixed value and patch *c* is 1 and $\sqrt{2}-1$. Exponential high pass filter function given by:

$$\hat{\mathrm{h}}(u,v) = \begin{cases} e^{\left[-a\left(\frac{d}{d\hat{}(u,v)}\right)^{k}\right]} & if\ (u,v) \neq (0,0) \\ 0 & if\ (u,v) = (0,0) \end{cases} \tag{5}$$

Fixed values of *a* is 1 and $\ln\sqrt{2}$ proposed by [18]. In this study, a high pass filter was applied to enhanced the edges of the image. Sample image of CT images, before and after high pass filter was applied are shown in Figure 4.

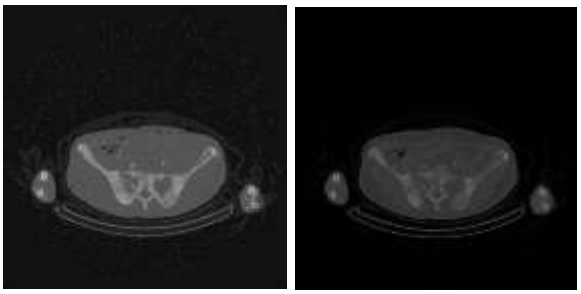

(a) (b)

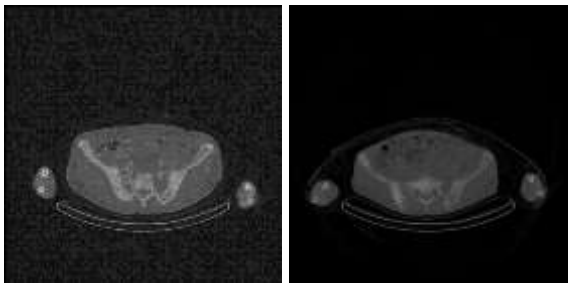

(c) (d)

Fig. 4: (a) and (c) are original images; (b) and (d) are output image with high pass filter 4.3 × 3.

2.2.3 Median filter

Median filter is a filter that smoothen a non-linear space. Median filters are also known as order statistics filters or rank order filters. When processing images, median filters use descending neighbourhoods and test *m* values through neighbourhood *n*, which is around the pixels for input and output can be determined. Median filter changes the middle pixel's value with the median of its circular neighbouring pixels [19]. Equality of median filter is as follows:

$$f\hat{}\,(x,y) = median_{(s,t)\in S_{xy}}\{g(s,t)\}\,, \tag{6}$$

where $f\hat{}\,(x,y)$ delegate value image *f* stored in any point *(x, y)*, S_{xy}: delegate set the coordinates in rectangular sub image in a window (window) size $m \times n$ which is centralized at the point *(x,y)*. $g(s,t)$ represent the original faulty image [20].
Original pixel value is including the calculation of the median. Median filter is fairly popular because median filter is able to provide the ability to reduce noise than linear smoothing filters for the same image size.
The combination of original image, high pass filter output image and a constant *C*=100 image brightness and sharpness were increased. This can be seen in Figure 5 where filtered image (b and d) has a finer edge for bones, as well as a better contrast for the rest of artefacts in the scanned images (a and c).

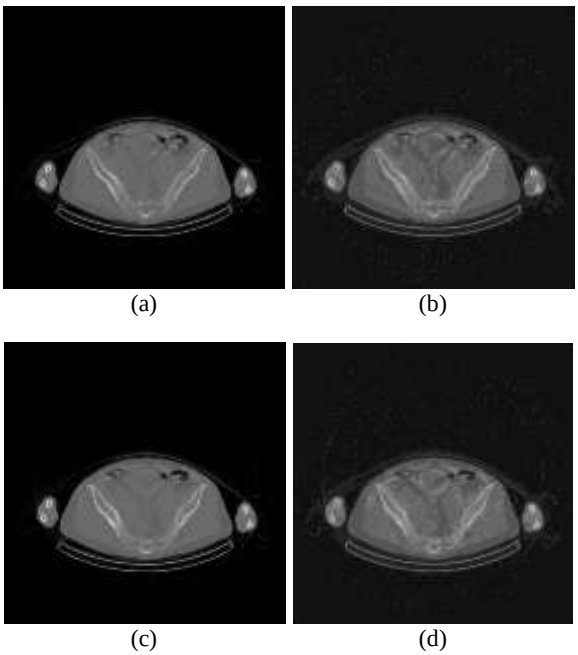

(a) (b)

(c) (d)

Fig. 5: (a), (c) and (e) are original images; (b), (d) and (f) are output images of equation 3.6 after using median filter kernel 3 × 3.

2.2.4 Otsu thresholding

In image processing and computer vision, autofill method is used automatically to present histogram based image thresholds or grey-scale image reduction to binary images. This algorithm also considers the images were on consists of two classes of pixels or histogram bi-modal (for example, background and background), then calculates the optimum threshold that separates two this class. Therefore, the combination of this separation (intra-class variance) is minimal.
Otsu method is search in depth to the threshold that minimizes intra-class variance (variance with class), and is defined as the sum of the weights of variance for both class;

$$\sigma_w^2(t) = \omega_1(t)\sigma_1^2(t) + \omega_2(t)\sigma_2^2(t) \tag{7}$$

Weights ω_i is the probabilities of the two classes separated by a threshold t ,and σ_i^2 are variances of these two classes.
Thus, minimizing the intra-class variance is the same as maximizing inter-class variance.

$$\sigma_b^2(t) = \sigma^2 - \sigma_w^2(t) = \omega_1(t)\omega_2(t)\left[\mu_1(t) - \mu_2(t)\right]^2 \quad (8)$$

Where the mean probability of class ω_i and mean class is μ_i which probability of class is $\omega_1(t)$ calculated from the Probability histogram as

$$\omega_1(t) = \Sigma_0^t p(i) \quad (9)$$

While min class is $\mu_1(t)$:

$$\mu_1(t) = \left[\Sigma_0^t p(i)\, x(i)\right] / \omega_1 \quad (10)$$

Where $x(i)$ is the middle value of the bin histogram i in simplicity, it can count $\omega_2(t)$ and μ_t to the right of the histogram for bins greater than t the probability of the class and the mean of the class can be calculated by iteration. This idea is an effective algorithmic result.

2.2.5 Region growing algorithm

The region-based algorithm is based on continuity. Using this technique, images are divided into sub-regions. The region-based technique depends on the pattern of intensity values alongside the neighbourhood pixel grouping. Each region is a grouping and the main goal of the algorithm is to aggregate regions according to the role of anatomy or function [21]. This method starts with the next pixel to add the pixel based on the similarity of the region. When the growing region stops on another (optional) pixel (pixels not available in the selected region) and the process goes on again. This process repeats until all pixels are included in a region.
This method works as multiple criteria can be selected at the same time. Thus, many image noises can be excluded, and finally, the relevant region can be found [17]. At this point, the main purpose is to find the brightest pixel in the image which identifies as suspicious. This is because it might represent the region of the tumour. The seed point value is set to 80 and the threshold to 90; based on experiments. Therefore, the point with a grey scale value of less than 90 and above from the optional point of 80 is chosen. Samples showing the result are shown in Figure 6.

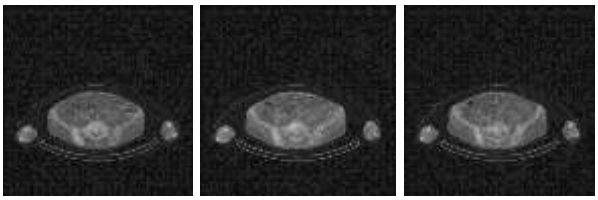

(a) (b) (c)

Fig.6: (a-c) Sample Segmentation with regional growth. Option point value of optional point value 80 and threshold of 90.

The seed point value is selected based on abnormal location based on region of the tumour that will be highest light in the image. These pixels are then used as the seed points of an image.

2.3 Classification

2.3.1 Feature extraction

A measurable technique for looking at texture that considers the spatial relationship of pixels is the grey-level co-occurrence matrix (GLCM), otherwise called the grey-level spatial dependence matrix. The GLCM capacities describe the surface of a picture by computing how regularly combines of pixel with particular qualities and in a predefined spatial relationship happen in an image, making a GLCM, and after that extricating factual measures from this matrix. The intensity histograms of an image or region are usually used to describe texture. The info gained from histograms calculation symbolize on the distribution of the intensities and nothing about the position relative between the pixels in that texture. Co-occurrence matrix is a good statistical approach which provides valuable info about the position relation of the neighbouring pixels in an image [22].
Given an image I, of size N×N, the co-occurrence, matrix P can be defined as.

$$P(i,j) =$$

$$\sum_{x=1}^{N}\sum_{y=1}^{N}\begin{cases}1, & if\ I(x,y) = i\ and\ I(x+\Delta x, y+\Delta y) = j \\ 0, & otherwise\end{cases} \quad (11)$$

where the offset (Δx, Δy) describes the distance between the pixel of interest and the surrounding neighbours. Because of this offset the co-occurrence matrix is sensitive to rotation. When selecting an offset vector in a way it does not rotate the image in 180 degree will lead to different outcome co-occurrence matrix for the same rotated image [23]. To avoid this problem by forming co-occurrence matrix using a set of offset sweeping through 180 degrees at the same distance parameter Δ to achieve a degree of rotational invariance (i.e., [0 Δ] for 0◦ :P horizontal, [-Δ, Δ] for 45◦ : P right diagonal, [-Δ 0] for 90◦ : P vertical, and [-Δ −Δ] for 135◦ : P left diagonal).
After producing a co-occurrence matrix, the image feature can be extracted from the original CT image combined with the output image for opening operation. The number of images feature extraction is as many as 21 features. Vectors of dimensions and discriminative powers are reduced by using Component Analysis (PCA). The PCA is effective in reducing data delimitation and also reducing the cost of computation of new data analysis [24].

2.3.2 Random forest

Estimation of error testing in Random forest are determined based on training sample during forest dispersion. Each non-selected sample in boot strap is called as OOB sample [25]. It uses OOB sample as input for tree matching during performing prediction (novel testing sample). According to kept calculation, the highest vote and average of regression will take into account for all OOB samples from all trees. Error testing estimation becomes more accurate during training process with inclusion of proper number of trees.
Several equations should be considered when categorizing Random Forest accuracy. For example, given a set of ensemble classifier. $h_1(x), h_2(x), \ldots, h_K(x)$, and training set randomly obtained from random vector distribution (X, Y), which defined as margin function mg as below:

$$mg(X,Y) = p_k In(h_k(X) = Y) - \max_{\{j \neq Y\}} p_k \, In(h_k(X) = j) \tag{12}$$

where $In(*)$ is indicator function that calculates the average number of voting, p at X, Y for true (normal) class more than average voting of other class (abnormal). The bigger margin, mg represents higher confidence of classification accuracy. Therefore, equation of generalization, RG is defined below:

$$RG^* = P_{X,Y}(mg(X,Y) < 0) \tag{13}$$

where (X, Y) is represents probability of denominator of (X, Y) space.

2.3.3 Logistic regression (LR)

LR Model is among the simplest model which uses linear function on feature parameter. Furthermore, some complex LR involving higher level terms, they describe the interaction between the feature parameters. First-command of LR model grabs P as conditional probability distribution, $P(Y = 1 \mid X)$ from parameter linear function perspective as below:

$$\left(\frac{P(Y=1 \mid X)}{1-P(Y=1 \mid X)}\right) = \alpha + \sum_{i=1}^{p} \beta_j X_j \tag{14}$$

where α and □□$_j$, j □□1,..., p, are estimated parameter. LR model prepares direct calculation of correlation probability posterior $P(Y \mid x)$ to the class parameter such as x (our case consider two classes namely normal or abnormal), by injecting feature parameter. Decision rule of LR model relies on posterior probability threshold. This threshold is derived from a set of wrongly classified in pelvis bone scan classification domain.

3. Result and Discussion

Objective of this experiment is to compare Random Forest and LR on pelvis bone scan classification system for prostate cancer proliferation. Both classifiers are chosen because they are no difference in significant test presented by [15]. Random Forest uses maximum depth of tree, slot behaviour number, number of features, number of trees and seed with 0,1, 10, 20 dan 1, in sequence. On the other hand, LR uses learning rate, similar number of iteration and number of vector with -1 dan 1.0E-8, respectively. Table 1(a) shows results of Random Forest and LR performance according to several split percentages in the range of 50 until 75.

Table 1: Accuracy rate and Root Mean Square Error of Random Forest and Logistic Regression in the range of 50 to 75 split percentage and (b) cross validation using k=10 and k=25

(a)

Classifier	Random Forest		Logistic Regression	
Split percentage	Accuracy rate	Root Mean Square Error	Accuracy rate	Root Mean Square Error
50	88	0.3086	93	0.2358
55	85	0.384	90	0.316
60	83	0.3637	91	0.2887
65	87	0.3314	96	0.1796
70	92	0.2650	96	0.1925
75	86	0.2747	95	0.2132
Average	86.83	0.3212	93.5	0.2376

(b)

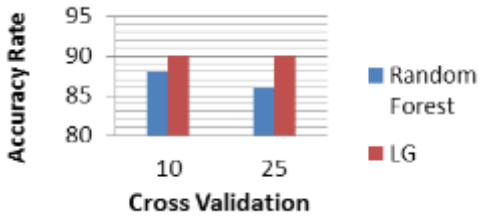

Based on Table 1(a), LR gains higher accuracy rates compared to Random Forest (approximately 96% and 92% with 70% split percentage). LR also shows stable performance than Random Forest as it produces lesser root mean square error (0.1925) than Random Forest (0.2650). This is further supported with the performance of these technique with 10 and 25 folds' validation techniques (as shown in Table 1(b)), where LR obtains higher performance in comparison to Random Forest. LR managed to achieve 90% accuracy in both 10-fold and 25-fold while Random Forest gains from 86 and 88 of accuracy rates.

Apart of diagnosing from bone scan images, this prostate cancer diagnosis model will also integrate expert rules in its inference engine. Here, a rule-based classification was carried out on patient data sets that have been prepared during pre-processing of data. Rules based classification technique used is the Random Tree classifier for pilot test.

Table 2: Accuracy rate and Root Mean Square Error for Random Tree

Classifier	Cross Validation	Accuracy rate	Logistic Regression
Random Tree	10	90	0.1617
	25	96	0.2393

Random Tree is a good machine learning classifier techniques as it has been trained using a variety of different parameters to see the capabilities of the technique in forecasting and making classifying. The results show that the random tree gives 96% accuracy for classification. In summary, LR outperforms Random Forest when classifying pelvis bone scan for prostate cancer recognition, while Random tree excels in classifying data from text input.

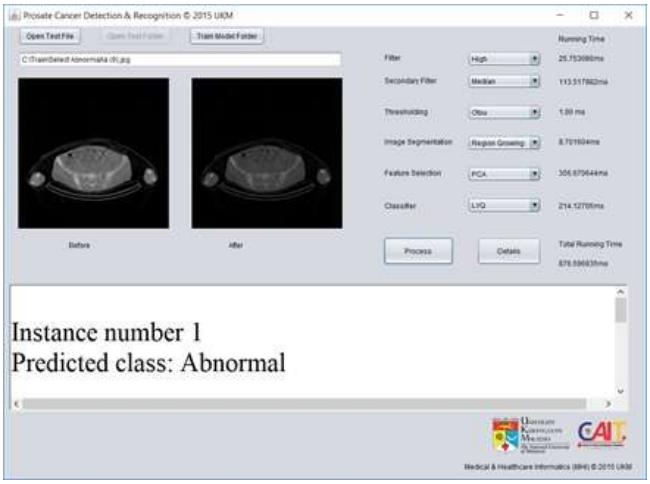

Fig.7: Main interface for classifying class normal or abnormal image.

Figure 7 shows the main interface of this expert system. Although the system is 96% accurate in classifying cancer cases, doctors can always overwrite the system recommendation as they were the experts. In addition, the main interface is also loaded with information on the accuracy of predictions in identifying cancer.

4. Conclusion

The implementation of LR in classifying bone scan images into normal and abnormal prostate cancer gives a better accuracy rate compared to the Random Forest approach, with insignificant increased of minimum error rate. This proves that this technique has the potential to offers automated high accuracy recognition of prostate cancer and indirectly saves time. In addition, this can be combined with other image and symptom modalities for faster diagnosis.

Acknowledgement

We would like to acknowledge the Fakulti Teknologi dan Sains Maklumat and UKM; for the facilities and financial support through research grants DIP-2015-023, FRGS/1/2016/ICT02/UKM/01/1 dan GGPM-2016-074.

References

[1] Zainal Ariffin Omar & Tamin, N. S. I., *National Cancer Registry Report 2007*, 2011.
[2] Fairul Asmaini Mohd Pilus, "Awas kanser prostat", *Newspaper of Harian Metro*, 2015. https://www.hmetro.com.my/node/23137.
[3] Denis Campbell, "Almost half of cancer patients diagnosed too late", *Newspaper of The Guardian*, 2014. https://www.theguardian.com/society/2014/sep/22/cancer-late-diagnosis-half-patients.
[4] CancerCare, "Prostate Cancer: Fourth Most Common Cancer Among Malaysian Men", AXA Affin, 2016. https://www.110cancercare.com/blog/prostate-cancer-fourth-most-common-cancer-among-malaysian-men-axa-cancercare-blog.html.
[5] M.J.P. Castanho, F. Hernandes, A.M. De Ré, S. Rautenberg & Billis, A, "Fuzzy expert system for predicting pathological stage of prostate cancer", *Journal of Expert Systems with Applications*, Vol. 40, No. 2, pp. 466-470, 2013.
[6] Murat Cinar, Mehmet Engin, Erkan Zeki Engin & Ateşçi, Y. Z., "Early prostate cancer diagnosis by using artificial neural networks and support vector machines", *Journal of Expert Systems with Applications*, Vol. 36, No. 3, pp.6357-6361, 2009.
[7] G. Lemaître, R. Martí, J. Freixenet, J. C. Vilanova, P. M. Walker, and F. Meriaudeau, "Computer Aided Detection and diagnosis for prostate cancer based on mono and multi-parametric MRI: A review", *Journal of Computer in Biology and Medicine*, Vol. 60, pp. 8-31, 2015.
[8] Adam A., Bulpitt A. and Treanor D., "Grading Dysplasia in Barrett's Oesophagus Virtual Pathology Slides with Cluster Co-occurrence Matrices", *In Proc. of Histopathology Image Analysis: Image Computing in Digital Pathology in conjunction with The 15th International Conference on Medical Image Computing and Computer Assisted Intervention (MICCAI)*, 2012.
[9] El-Dahshan, E., Salem, A. B. M. and Younis, T. H., "A Hybrid Technique for Automatic MRI Brain Images Classification", *Studia Univ. Babes-Bolyai, Informatica*, Vol. 54, No.1, pp. 55-67, 2009.
[10] Yazan M. Alomari, Siti Norul Huda Sheikh Abdullah, Reena Rahayu Md Zin, Khairuddin Omar, "Iterative randomized irregular circular algorithm for proliferation rate estimation in brain tumor Ki-67 histology images", *Journal of Expert Systems with Applications*, Vol. 48, pp.111-129, 2016.

[11] Dheeb Albashish,Shahnorbanun Sahran, Azizi Abdullah,Afzan Adam, Nordashima Abd Shukor,Suria Hayati Md Pauzi, "Multi-scoring feature selection method based on SVM-RFE for prostate cancer diagnosis", *The 5th International Conference on Electrical Engineering and Informatics 2015* , pp. 682-686, 2015.
[12] Alomoush, WK., Abdullah, S. N. H. S., Sahran, S. & Hussain, R. I., "Segmentation of MRI brain images using FCM improved by firefly algorithms", *Journal of Applied Sciences*, Vol. 14, pp. 66-71, 2014.
[13] Kaidar, S. M., Hussain, R. I., Bohani, F. A., Sahran, S., binti Zainuddin, N., Ismail, F., Thanabalan, J., Kalimuthu, G. & Abdullah, S. N. H. S., "Brain tumor treatment advisory system", *Journal of Soft Computing Applications and Intelligent Systems*, pp. 78-88, 2013.
[14] W. N. A. Baharuddin,S. N. H. S. Abdullah, S. Sahran, A. Qasem, A. bin Abdullah R. Iqbal, F. Ismail, "Type 2 Fuzzy Logic for mammogram breast tissue classification", *International Conference on Industrial Informatics and Computer Systems (CIICS)*, pp. 1-6, 2016.
[15] Siti Norul Huda Sheikh Abdullah, Farah Aqilah Bohani, Baher H. Nayef, Shahnorbanun Sahran, Omar Al Akash, Rizuana Iqbal Hussain, and Fuad Ismail, "Round Randomized Learning Vector Quantization for Brain Tumor Imaging", *Journal of Computational and Mathematical Methods in Medicine*, Vol. 2016, p. 19, 2016.
[16] Ponraj, D. N., Jenifer, M. E., Poongodi, P. and Manoharan, J. S., "Morphological Operations for the Mammogram Image to Increase the Contrast for the Efficient Detection of Breast Cancer", *European Journal of Scientific Research*, Vol. 68, No. 4, pp. 494-505, 2012.
[17] Shaoqing, Z. and Lu, X., "The Comparative Study of Three Methods of Remote Sensing Image Change Detection", *Proceedings of ISPRS Congress*, Istanbul, Turkey, pp.12-23, 2008.
[18] Wilson, G. X. R. J. N., *Handbook of Computer Vision Algorithms in Image Algebra CRC Press*, CRC Press LLC, 1996.
[19] Patnaik, C. S. P. a. S., "Filtering Corrupted Image and Edge Detection in Restored Grayscale Image Using Derivative Filters", *International Journal of Image Processing 3*, pp. 105-119, 2009.
[20] Gupta, G., "Algorithm for Image Processing Using Improved Median Filter and Comparison of Mean, Median and Improved Median Filter", *International Journal of Soft Computing*, Vol. 1, No. 5, pp. 304-311, 2011.
[21] Punamthakare, "A Study of Image Segmentation and EdgeDetection Techniques", *International Journal on Computer Science and Engineering*, Vol. 3, No.2, pp. 6, 2011.
[22] Eleyan, A. and Demirel, H., "Co-Occurrence Matrix and Its Statistical Features as a New Approach for Face Recognition", *Turkish Journal of Electrical Engineering and Computer Sciences*, Vol. 19, No. 1, pp. 97-107, 2011.
[23] Dougherty, E.R. dan LotufoR.A., "Hands-on morphological image processing", *SPIE-International Society for Optical Engineering*, Washington, USA, 2003.
[24] El-Dahshan, E., Salem, A. B. M. and Younis, T. H., "A Hybrid Technique for Automatic MRI Brain Images Classification", Studia *Univ. Babes-Bolyai, Informatica*, Vol. 54, No.1, pp. 55-67, 2009.
[25] Breiman, L., *Random forest*, Kluwer Academic Publishers, pp. 5-32, 2001.